



Solid solution softening or hardening induced by minor substitutional additions in a Hf₂₀Nb₃₁Ta₃₁Ti₁₈ refractory high entropy alloy

Downloaded from: <https://research.chalmers.se>, 2025-07-02 06:01 UTC






Citation for the original published paper (version of record):

Li, X., Jin, L., Mao, H. et al (2023). Solid solution softening or hardening induced by minor substitutional additions in a Hf₂₀Nb₃₁Ta₃₁Ti₁₈ refractory high entropy alloy. AIP Advances, 13(8).
<http://dx.doi.org/10.1063/5.0160762>

N.B. When citing this work, cite the original published paper.

RESEARCH ARTICLE | AUGUST 28 2023

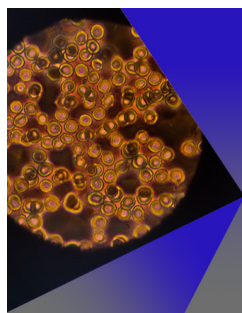
Solid solution softening or hardening induced by minor substitutional additions in a $\text{Hf}_{20}\text{Nb}_{31}\text{Ta}_{31}\text{Ti}_{18}$ refractory high entropy alloy

Xiaolong Li ; Lu Jin; Huahai Mao ; Hideyuki Murakami ; Sheng Guo  

AIP Advances 13, 085033 (2023)

<https://doi.org/10.1063/5.0160762>View
OnlineExport
Citation

CrossMark

**AIP Advances**Special Topic: Medical Applications
of Nanoscience and Nanotechnology**Submit Today!**

Solid solution softening or hardening induced by minor substitutional additions in a $\text{Hf}_{20}\text{Nb}_{31}\text{Ta}_{31}\text{Ti}_{18}$ refractory high entropy alloy

Cite as: AIP Advances 13, 085033 (2023); doi: 10.1063/5.0160762

Submitted: 12 June 2023 • Accepted: 1 August 2023 •

Published Online: 28 August 2023



Xiaolong Li,¹ , Lu Jin,^{2,3} Huahai Mao,⁴ , Hideyuki Murakami,^{2,5} and Sheng Guo^{1,a)}

AFFILIATIONS

¹ Department of Industrial and Materials Science, Chalmers University of Technology, Gothenburg SE-41296, Sweden

² Research Center for Structural Materials, National Institute for Materials Science, Sengen 1-2-1, Tsukuba, Ibaraki 305-0047, Japan

³ Division of Materials Science and Engineering, Graduate School of Shibaura Institute of Technology, Tokyo 135-8548, Japan

⁴ Thermo-Calc Software AB, Råsundavägen 18A, SE-169 67 Stockholm, Sweden

⁵ Department of Nanoscience and Nanoengineering, Waseda University, 3-4-1 Okubo Shinjuku, Tokyo 169-8555, Japan

^{a)} Author to whom correspondence should be addressed: sheng.guo@chalmers.se

ABSTRACT

The effect of minor additions of substitutional elements such as Al, Cu, Mn, and Fe on the room-temperature (RT) and elevated-temperature hardness of a single bcc phase $\text{Hf}_{20}\text{Nb}_{31}\text{Ta}_{31}\text{Ti}_{18}$ refractory high entropy alloy is studied here. Interestingly, 2.5 at. % nominal addition of Fe hardened the base $\text{Hf}_{20}\text{Nb}_{31}\text{Ta}_{31}\text{Ti}_{18}$ alloy in the temperature range from RT to 800 °C, while the same nominal content of addition of Al, Cu, and Mn softened the base alloy from RT to 1000 °C. Regardless of solid solution hardening or solid solution softening, the hardness variation with temperature essentially showed the same three-stage pattern for all studied alloys here: a temperature-dependent decrease in hardness below 300 °C/400 °C, followed by a temperature-independent hardness plateau between 300/400 and 800 °C, and finally a temperature-dependent decrease in hardness at temperatures higher than 800 °C. The mechanism for solid solution hardening or softening in bcc-structured refractory high entropy alloys is discussed, together with their temperature dependence.

© 2023 Author(s). All article content, except where otherwise noted, is licensed under a Creative Commons Attribution (CC BY) license (<http://creativecommons.org/licenses/by/4.0/>). <https://doi.org/10.1063/5.0160762>

I. INTRODUCTION

Refractory high entropy alloys (RHEAs) have been attracting increasing attention from the materials community since their first discovery in 2010 by Senkov *et al.*^{1,2} With a yield stress of above 400 MPa at 1600 °C for some RHEAs, it is not surprising that they are widely regarded as promising replacements for the state-of-the-art Ni-based superalloys in high-temperature (HT) applications, e.g., jet engines. Currently, the upper bound of working temperature for jet engines using Ni-based superalloys is lower than 1500 °C, set by their melting points (T_m). An almost 50% increase in output power for future jet engines could result from operating at around 1300 °C without auxiliary cooling.³ Continuous efforts from the materials perspective have been made to push jet engines to operate at higher temperatures for increased energy efficiency. Examples include covalent bond based intermetallics or ceramics,

which are known to possess excellent chemical stability and HT strength. They, however, typically suffer from brittleness, especially at room temperature (RT), which significantly restricts their manufacturing and processing. Another example is refractory metals or alloys with high T_m , but with a metallic bond instead. Particularly, Nb-based alloys stand out among refractory alloys with several merits that are suitable for HT applications: high T_m (2469 °C for Nb), comparable density (8.57 g/cm³) to Ni-based superalloys, and ductile–brittle transition temperature (DBTT) lower than RT. However, compared to Ni-based superalloys, the strength of Nb alloys needs much improvement, especially at HT.⁴ Solid solution hardening (SSH)⁵ is no doubt one strategy applicable to strengthen Nb alloys, without worrying much about embrittlement that is typically accompanied by secondary phase strengthening. Unfortunately, the hardening effect from SSH is rather limited in traditional solid solutions. The concept of high entropy alloys (HEAs)^{6–9} brings new

opportunity for SSH.¹⁰ The alloying strategy of HEAs also greatly expands the compositional space, which was previously defined by the conventional alloy design and limited to the corners of phase diagrams. Some claimed advantages of HEAs include the high entropy effect to stabilize the solid solution phase(s),¹¹ the severe lattice distortion effect, which is closely related to SSH, and the controversial sluggish diffusion effect,¹² which could contribute to enhanced thermal stability. Eventually, the combination of refractory alloys such as Nb alloys, and the alloy design strategy of HEAs, created a new category of alloys, RHEAs, a highly pursued field of research in the domain of HEAs and the topic of the current work.

For alloys aiming for HT applications, they require to simultaneously possess high strength at HT and sufficient tensile ductility at RT. These material requirements are much more demanding than the material requirements to conquer the well-known trade-off between strength and ductility at RT.¹³ As a new type of HT materials, RHEAs are now facing the same challenge. For example, the SSH strategy has been proved to work nicely to enable excellent HT strength for single bcc phase RHEAs,^{14–17} but all at the cost of tensile ductility at RT. The other strategy is to start with RT tensile ductile RHEAs and then to strengthen them by SSH or by coherent secondary phases, as in the case of Ni-based superalloys. For example, ductile RHEAs such as HfNbTaTiZr and their derivatives^{14–16} have been extensively explored, but they all showed rather low strength at HT,¹⁷ benchmarked by Ni-based superalloys. Using the SSH strategy, the HT strength of some originally ductile RHEAs could be enhanced by doping a high-level addition of Mo or W, but that unfortunately led to embrittlement of the alloys. Inspired by the coherent γ/γ' microstructure in Ni-based superalloys, there existed some efforts to obtain a coherent B2/bcc microstructure in RHEAs.^{18–20} Typically, the spinodal decomposition between Zr and Ta (Nb) at HT^{21,22} was utilized, Al was added to order the Zr-enriched bcc phase into the B2 phase, a large lattice misfit between two phases (BCC and B2) was generated, and in some cases, a reversible inversion of them was triggered.^{23,24} The thermal instability of superalloys such as RHEAs containing a coherent bcc/B2 structure, however, remains a major concern especially at HT.^{24,25} After reviewing the HT strength of reported single-phase and multi-phase RHEAs,¹⁷ Senkov *et al.* concluded that compared to multi-phase RHEAs, SSH-ed single bcc phase RHEAs with high T_m and naturally also high density have better thermal stability and a higher chance to retain their strength at higher temperatures. At $T \geq 0.6T_m$, as the diffusion-controlled deformation mechanism is likely activated, a quick drop in strength is expected for single-phase RHEAs. To summarize, how to achieve RT ductility without compromising HT strength and thermal stability is still a formidable challenge to push forward the alloy development of RHEAs.

One now considers strategies to soften those alloys with decent HT strength but poor RT ductility, for example, the previously mentioned single bcc phase RHEAs with high T_m . It must be noted that RT ductility that can be expected for RHEAs with decent HT strength would be marginal, but certainly not zero. Contrary to the SSH strategy, solid solution softening (SSS), which is a well-documented phenomenon mainly existing in bcc structured materials,^{26,27} can be utilized to soften the alloys at RT to induce ductility. As examples, Mo and W with higher DBTT than RT, can be ductilized by alloying with elements such as Re and Os.^{26–29} SSS was indeed a rather extensively studied research topic with the following

distinct features revealed:^{30–32} it predominately affects flow stress at low temperatures, i.e., below $0.15T_m$,^{37,38} both interstitial and substitutional solutes can induce SSS.³¹ However, due to the high cost and scarcity of elements such as Re or Os, the application of the SSS strategy in dilute refractory alloys (compared to RHEAs with concentrated alloy compositions) was limited. Interestingly, based on the first-principles calculations, cost effective Al and Mn were predicted to be the most promising alternatives to Re to improve the ductility of W at low temperatures, among 21 substitutional alloying elements that were investigated.³³ Inspired by the theoretical efforts, we therefore propose to employ the SSS strategy to induce RT ductility in RHEAs by alloying with elements such as Mn and Al. The hope is that alloying can trigger SSS at RT while the HT strength can be at least retained, if not enhanced. Ultimately, we intend to apply this strategy for those RHEAs with decent HT strength but poor RT ductility. However, to prove the concept, here, we start from RHEAs with some RT ductility (and naturally not superior HT strength) as a continuation of our previous research line working with ductile RHEAs.¹⁵

II. METHODS

RHEAs with nominal compositions of $\text{Hf}_{20}\text{Nb}_{31}\text{Ta}_{31}\text{Ti}_{18}$ (denoted as HNTT) and $\text{Hf}_{20}\text{Nb}_{29.75}\text{Ta}_{29.75}\text{Ti}_{18}\text{-X}_{2.5}$ ($X = \text{Mn, Al, Cu, and Fe}$, denoted as HNTT-Mn, HNTT-Al, HNTT-Cu, and HNTT-Fe, respectively) in at. % were arc-melted using high purity (>99.95%) elements at least five times to ensure chemical homogeneity followed by furnace cooling. The nominal content of doped alloying elements was fixed to be 2.5 at. %, to separate the effect of the micro-alloying level on SSH or SSS. Regarding the choice of alloying elements, Mn and Al were selected based on the first-principles calculation results, as stated previously, while others were added mainly for comparison purposes. The microstructure and local chemical compositions were measured using a field emission gun scanning electron microscope (FEGSEM, LEO-1550) equipped with a backscatter electron (BSE) detector and by energy dispersive spectroscopy (EDS). As can be seen from Table I, there were some losses in metals with low melting points (compared to those of refractory elements) during melting, and particularly, the loss of Mn was rather significant due to the high volatilization of Mn and a long melting time (>2 min per melting) at over 450 mA of the arc melting current. The crystal structure was tested using an x-ray diffractometer (XRD, Bruker D8 Advance) using $\text{Cu-K}\alpha_1$ radiation in the two theta range of 20° to 100° . The hardness from RT to 1000°C was tested using a high temperature Vickers hardness tester (Intesco-HTM 1400) under high-vacuum (down to 2.0×10^{-5} Pa), with a load

TABLE I. Measured compositions of the tested alloys by EDS, in at. %.

Alloy ID	Nb	Ta	Hf	Ti	Mn	Al	Cu	Fe
HNTT	31.1	30.6	20.8	17.6				
HNTT-Mn	29.2	30.8	22.0	17.8	0.2			
HNTT-Al	29.0	30.8	20.6	17.7		1.9		
HNTT-Cu	30.2	29.8	21.0	17.6			1.3	
HNTT-Fe	28.6	29.9	20.9	18.1				2.4

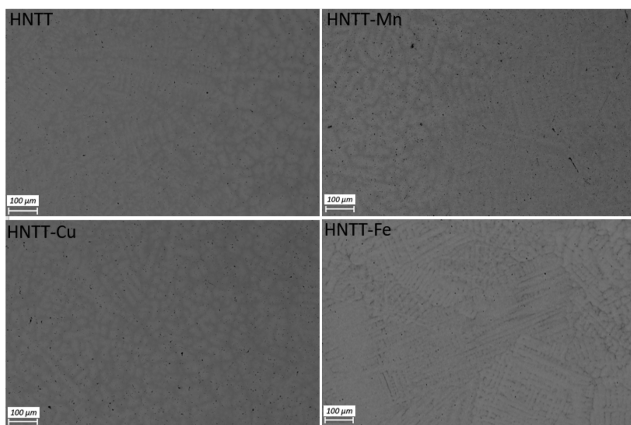


FIG. 1. BSE images of as-cast HNTT, HNTT-Mn, HNTT-Cu, and HNTT-Fe alloys.

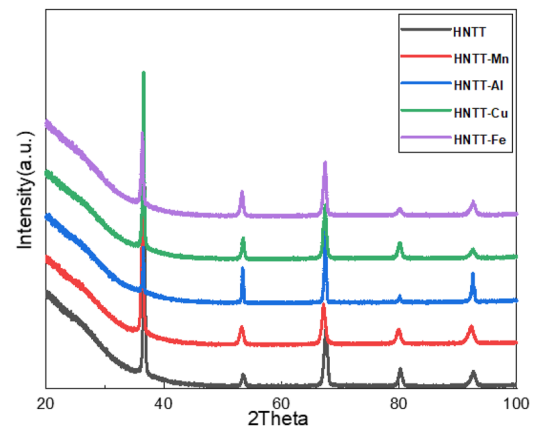


FIG. 3. XRD patterns of HNTT, HNTT-Mn, HNTT-Al, HNTT-Cu, and HNTT-Fe alloys.

of 1.0 kgf and a dwell time of 10 s. The hardness value was averaged from around five indentations at each temperature.

III. RESULTS

Figure 1 shows the microstructures of HNTT, HNTT-Mn, HNTT-Cu, and HNTT-Fe alloys, where dendritic and interdendritic features typically seen in directly cast HEAs were observed. An EDS elemental mapping of the HNTT-Al alloy, given in Fig. 2, shows the segregation of Ta with high T_m in the dendritic region and segregation of Ti and Al with relatively low T_m in the interdendritic region, and the same pattern was seen in all the alloys tested here (not shown for simplicity). All the tested alloys were identified to be of the single bcc phase, according to Fig. 3, which was intended for the purpose of studying SSH or SSS in this work.

The Vickers hardness for all the tested alloys, at temperatures ranging from RT to 1000 °C, is given in Table II and plotted in

Fig. 4. Essentially, all the alloys showed a three-stage pattern, reminiscent of how the flow stress varies as a function of temperature in RHEAs and other bcc structured materials.^{34–36} First, at low temperatures below 300 °C (400 °C for HNTT-Fe), the hardness was strongly influenced by the temperature and different substitutional solutes. Normally, the lower the temperature, the higher the hardness, which was also the scenario seen in this case. With 2.5 at. % nominal addition of Mn, Al, and Cu, the HNTT base alloy was softened by 20%, 18.1%, and 13.3%, respectively, while 2.5 at. % nominal addition of Fe instead hardened HNTT by 5.2%. Second, at intermediate temperatures ranging from 300 °C (400 °C for HNTT-Fe) to 800 °C, the hardness was almost stabilized, and a plateau was seen. Finally, at high temperatures over 800 °C, the hardness of all the alloys dropped quickly, presumably due to the increasing impact of thermally diffusion-controlled processes. We will not pay much attention to this temperature range since it does not help with the

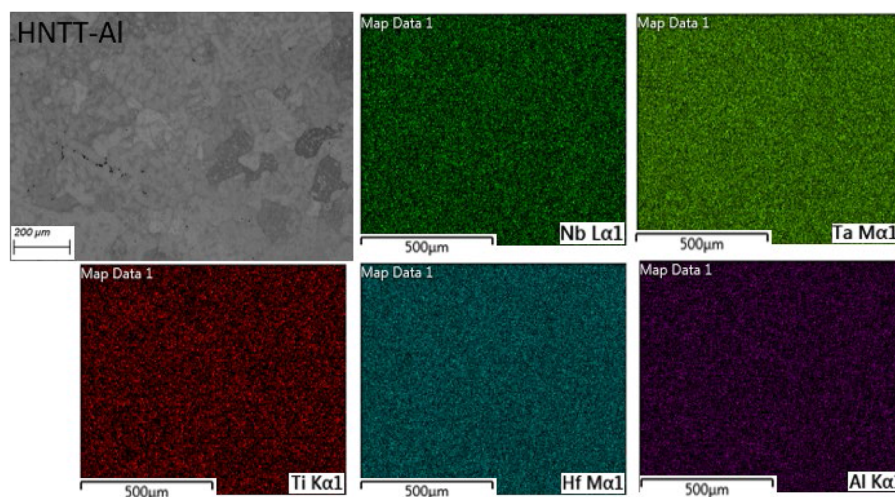
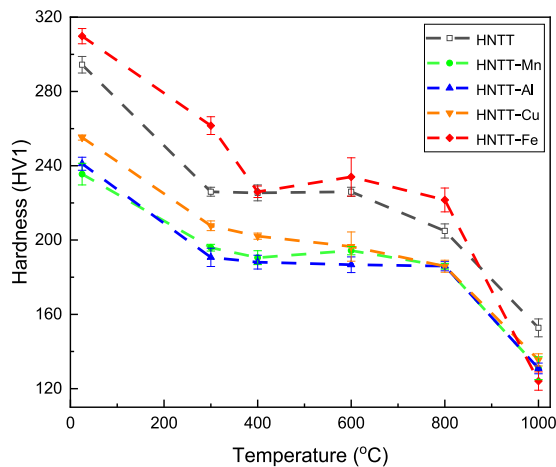


FIG. 2. EDS elemental mapping of the HNTT-Al alloy.

TABLE II. Vickers hardness of HNTT, HNTT-Mn, HNTT-Al, HNTT-Cu, and HNTT-Fe alloys at various temperatures (in °C).

Alloy ID/ temperature	RT	300	400	600	800	1000
HNTT	294.4 ± 4.5	226.0 ± 2.4	225.4 ± 4.3	226.0 ± 2.5	204.9 ± 3.8	152.7 ± 4.8
HNTT-Mn	235.5 ± 5.8	195.9 ± 1.8	190.5 ± 3.8	194.3 ± 2.2	185.9 ± 1.6	131.0 ± 6.1
HNTT-Al	241.1 ± 3.5	190.7 ± 4.9	188.1 ± 3.7	186.7 ± 4.2	186.0 ± 2.5	130.9 ± 2.9
HNTT-Cu	255.2 ± 1.4	207.7 ± 2.6	202.1 ± 1.7	196.5 ± 7.9	185.9 ± 3.2	135.5 ± 3.3
HNTT-Fe	309.8 ± 4.1	261.6 ± 4.8	226.0 ± 3.1	234.0 ± 10.3	221.6 ± 6.4	124.1 ± 4.9

**FIG. 4.** Temperature-dependent Vickers hardness for HNTT, HNTT-Mn, HNTT-Al, HNTT-Cu, and HNTT-Fe alloys.

discussion on achieving a decent HT strength. It is noted that at 1000 °C, the hardness of the HNTT-Fe alloy, with hardness higher than that of HNTT up to 800 °C, was lower than that of HNTT, indicating the loss of SSH at this temperature.

IV. DISCUSSION

We now try to rationalize the hardness variation for the tested RHEAs, as a function of temperature, based on the previous understanding on temperature dependent flow stress in bcc structured materials. Flow stress is known to be temperature dependent in bcc structured materials, and it is composed of two components: a thermal one, called effective stress, and an athermal one, known as the athermal stress.³⁷ Only effective stress is altered by SSS, with reduced temperature dependence when the temperature increases, at low temperatures. Athermal stress is governed by SSH at elevated temperatures, and it is generally constant and basically only affected by the lattice misfit due to atomic size and modulus differences, controlling how dislocations can move across. The barrier that gives rise to effective stress is of a short-range nature, while that for athermal stress is of a long-range nature. Therefore, these two components of the flow stress would interact with dislocations differently upon alloying.³⁷ Since the hardening mechanisms other than solid solution hardening can be ignored in these single-phase alloys, and the

hardness is in general linearly proportional to the strength, the temperature dependent hardness seen here naturally led us to infer that the hardness in RHEAs also consists of two components: effective hardness and athermal hardness.

We start from the first stage of the hardness variation, where in all the tested alloys, the hardness decreased with increasing temperature below 300 °C (400 °C for HNTT-Fe). Importantly, compared to the base HNTT alloy, HNTT-Fe showed a higher hardness while HNTT-Mn, HNTT-Al, and HNTT-Cu all showed a lower hardness at this temperature range. Apparently, a nominal 2.5 at.% addition of Fe led to SSH, while the same nominal content of Mn, Al, and Cu addition led to SSS in the base HNTT alloy. Softening or hardening effects in bcc structured materials are essentially produced by the interaction between solutes and the non-planar core of $1/2\langle 111 \rangle$ screw dislocations. There are two critical shear stresses that are responsible for the motion of these screw dislocations under the applied external stress: Peierls–Nabarro (P–N) stress, which will be maintained when the external stress is removed and is sensitive to the chemical environment of the screw dislocation core, and the stress to enable screw dislocations to advance forward.²⁶ P–N stress is associated with double-kink nucleation, which can accommodate screw dislocations and hence induce softening. This process forms spontaneously according to the lowest energy principle. The stress to move screw dislocations forward is associated with the kink migration process moving laterally along the dislocation line, which triggers hardening. Both processes are thermally activated, and their rates can be described by the Arrhenius equation as (attempt frequency) $\times \exp[-(\text{enthalpy barrier})/(k_B T)]$, where k_B is Boltzmann's constant and T is the temperature.²⁷ The enthalpy barriers have a stress scale and an energy scale,²⁷ both of which can be affected by the addition of solutes in a solid solution. The stress scale is correlated with the P–N stress and the stiffness for moving a single atomic row in the dislocation core, which changes with solutes since they change the stiffness, while the energy scale is connected to the direct solute–dislocation core interaction.²⁷ Temperature, of course, influences the thermally activated processes and hence both double-kink nucleation and kink migration. These two competing mechanisms are therefore affected by substitutional solute additions due to their effect on changing the enthalpy barrier and temperature, and their competition decides the ultimate softening or hardening behavior. Figure 5 shows a schematic illustration of two competing plastic deformation mechanisms between double-kink nucleation and kink migration in bcc structured alloys. Minor additions of Mn, Al, Cu, and Fe into the HNTT alloy shall improve the double-kink nucleation rate, regardless of the attractive or repulsive interactions

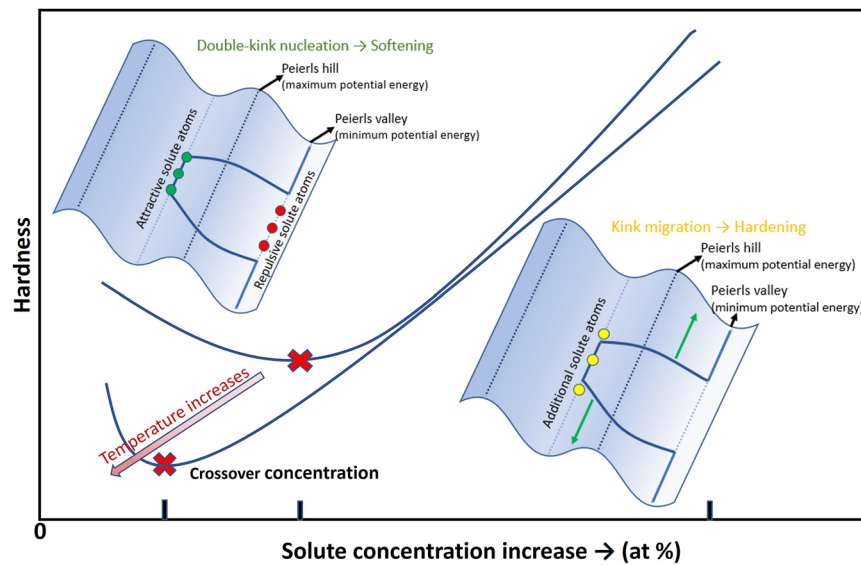


FIG. 5. A schematic illustration of two competing plastic deformation mechanisms between double-kink nucleation and kink migration in single phase bcc structured alloys at low temperatures. The cross-over concentration, from the double-kink nucleation dominated mechanism to the kink migration dominated mechanism, shifts to the lower concentration side when the temperature increases.

between different type of solutes and screw dislocations, and lead to softening. Both attractive and repulsive interactions could reduce the nucleation barrier along an initial straight dislocation line by pulling in or pushing away from the solute.³⁸ In this work, from RT to 300 °C, compared to the base HNTT alloy, the plastic deformation mechanism of alloys with 2.5 at. % nominal addition of Mn, Al, and Cu is double-kink nucleation dominated, leading to softening, and it is expected that the plastic deformation mechanism would transit to kink migration, which dominates when increasing the content of alloying additions, finally leading to hardening (confirmed and not shown here). Furthermore, considering that the base HNTT alloy has a hardness of 294 at RT, which is already quite soft, the softening effect here is distinct especially by Mn. Other factors potentially contributing to softening may include the addition of certain solutes constricting the extended core of screw dislocations, therefore facilitating the dislocation motion or an increased mobile dislocation density.^{26,39} However, for the alloy with the same nominal addition of Fe and at the same temperature range, it shall be kink migration dominated. Thus, adequate Fe atoms are already interacting with the dislocations along the dislocation line and prohibiting the lateral motion of kinked screw dislocations, leading to hardening. There exists a crossover concentration of the substitutional solute, below which the double-kink nucleation mechanism dominates so that softening occurs and above which the kink migration mechanism dominates so that hardening occurs. The crossover concentration shifts to the lower side with an increase in temperature since higher temperature helps accelerate double-kink nucleation more than kink migration. Thus, it can be concluded that softening or hardening in bcc structured alloys can be varied depending on the type and content of addition solutes, as well as the temperature range.

We then move to the second stage of the hardness variation, at intermediate temperatures ranging from 300 °C (400 °C for HNTT-Fe) to 800 °C, where the hardness was almost insensitive to temperature in all the tested alloys. In this case, the plasticity is mainly mediated by the Peierls motion and cross-slip of screw dislocations passing by the rough landscape resulting from the lattice misfit with collapses of edge dislocation dipoles at screw dislocations because of a strong self-diffusion under the applied shear stress.^{40–42} The scenario fits into the SSH mechanism, which comes from the elastic stress field generated from the interaction between dislocations and solute atoms.^{5,43} For a concentrated solid solution, the solute-induced stress increase, $\Delta\sigma$, can be expressed as $\Delta\sigma = A\mu\delta^{4/3}c^{2/3}$,⁴⁴ where A is a dimensionless constant, c is the content of solutes, and δ is the misfit parameter. This expression was initially developed for binary solid solutions with the concentration of the solvent exceeding 60%–70% and was subsequently modified and applied by Senkov *et al.* to the HfNbTaTiZr RHEA.¹⁴ Therefore, a direct correlation between yield stress (or hardness) and misfit parameters could be established for single phase bcc structured alloys, with the interaction force F increasing with an increase in the atomic size and modulus misfit between solutes and the solvent. The Vickers hardness of the studied alloys at 600 °C is used to illustrate the situation. The base HNTT alloy with a hardness of 226 at 600 °C was hardened by a nominal 2.5 at. % addition of Fe to a hardness of 234, while it was softened by the same nominal addition of Mn, Al, or Cu to hardness values of 194, 187, and 197, respectively. In principle, at intermediate temperatures, any addition of solutes into the base alloy would cause lattice distortion, generating the elastic stress field either due to the atomic size mismatch (smaller atomic size of transition metals than refractory elements) or the modulus misfit. However, the softening effect induced by the

addition of a minor amount of Mn, Al, and Cu was rather significant: around 20%, 18.1%, and 13.3%, respectively, at RT and around 14%, 17.4%, and 13.1%, respectively, at 600 °C. Therefore, the marginal hardening effect (around 6%, 0.7%, and 0.2% calculated using the actual Mn, Al, and Cu content, respectively, given in Table I) was overridden by the overall softening effect that was dominating in HNTT-Mn, HNTT-Al, and HNTT-Cu alloys. In addition, according to a recent finding, there is a possible transition in the strengthening mechanism from the screw dislocation dominated mechanism to edge dislocation dominated mechanism, depending on misfit parameters,⁴⁵ and edge dislocation-dominated alloys are more likely to retain the strength at higher homologous temperatures.⁴⁶ Therefore, the competition between hardening and softening can also be interpreted from different perspectives, which is out of the scope of this work. At this stage, we conclude that this athermal plateau is primarily controlled by SSH, which is influenced by lattice misfit.

V. CONCLUSION

In summary, minor additions of substitutional elements could cause either solid solution hardening or softening in a $\text{Hf}_{20}\text{Nb}_{31}\text{Ta}_{31}\text{Ti}_{18}$ RHEA, in a wide temperature range. 2.5 at. % nominal addition of Fe led to solid solution hardening due to a kink migration dominated plastic deformation mechanism, while the same nominal content of addition of Mn, Al, and Cu caused solid solution softening due to a double-kink nucleation dominated plastic deformation mechanism. A crossover of the dominating plastic deformation mechanism from double-kink nucleation to kink migration could be varied by the type and content of solutes added, as well as the temperature range. On the other hand, for all the studied alloys, regardless of the occurrence of solid solution hardening or softening, the hardness variation with temperature showed the same three-stage pattern: a temperature dependent hardness reduction from room temperature to 300 °C/400 °C, followed by an athermal plateau from 300/400 to 800 °C, influenced mainly by misfits in the atomic size and modulus, and finally a quick drop in hardness above 800 °C due to the enhanced diffusion-controlled processes. In the future, we plan to trigger solid solution softening that we revealed here in this work, to enable some tensile ductility (even marginal) at RT, for those bcc-structured RHEAs showing decent HT strength yet zero tensile ductility, by engineering the type and content of substitutional additions. Meanwhile, we also intend to actively learn from what large-scale density functional theory (DFT) and density functional tight binding (DFTB) calculations could provide to guide the alloy design of HEAs, including RHEAs, and importantly to optimize their mechanical behavior.^{47,48}

ACKNOWLEDGMENTS

X.L.L. and S.G. thank the Swedish Research Council (Grant No. 2019-03559) for the financial support. X.L.L. is also grateful for the financial support from the JSPS (Japan Society for the Promotion of Science) Summer Program and the Axel Hultgrens Fund. The authors would like to thank Professor Yoko-Yamabe-Mitarai at the University of Tokyo and Professor Nobuhiro Tsuji at Kyoto University for the useful suggestions and discussions.

AUTHOR DECLARATIONS

Conflict of Interest

The authors have no conflicts to disclose.

Author Contributions

Xiaolong Li: Conceptualization (equal); Data curation (equal); Formal analysis (equal); Investigation (equal); Validation (equal); Writing – original draft (equal). **Lu Jin:** Investigation (equal); Methodology (equal); Resources (equal); Writing – review & editing (equal). **Huahai Mao:** Writing – review & editing (equal). **Hideyuki Murakami:** Methodology (equal); Resources (equal); Writing – review & editing (equal). **Sheng Guo:** Conceptualization (equal); Funding acquisition (equal); Project administration (equal); Supervision (equal); Writing – review & editing (equal).

DATA AVAILABILITY

The data that support the findings of this study are available from the corresponding author upon reasonable request.

REFERENCES

- O. N. Senkov, G. B. Wilks, D. B. Miracle, C. P. Chuang, and P. K. Liaw, *Intermetallics* **18**, 1758–1765 (2010).
- O. N. Senkov, G. B. Wilks, J. M. Scott, and D. B. Miracle, *Intermetallics* **19**, 698–706 (2011).
- J. H. Perepezko, *Science* **326**, 1068–1069 (2009).
- V. V. Satya Prasad, R. G. Baligidad, and A. A. Gokhale, “Niobium and other high temperature refractory metals for aerospace applications,” in *Aerospace Materials and Material Technologies*, Indian Institute of Metals Series, edited by N. E. Prasad and R. J. H. Wanhill (Springer, Singapore, 2017), pp. 267–288.
- T. Suzuki, *Jpn. J. Appl. Phys.* **20**, 449 (1981).
- Y. Zhang, T. T. Zuo, Z. Tang, M. C. Gao, K. A. Dahmen, P. K. Liaw, and Z. P. Lu, *Prog. Mater. Sci.* **61**, 1–93 (2014).
- D. B. Miracle and O. N. Senkov, *Acta Mater.* **122**, 448–511 (2017).
- O. N. Senkov, D. B. Miracle, K. J. Chaput, and J. P. Couzinie, *J. Mater. Res.* **33**, 3092–3128 (2018).
- F. Maresca and W. A. Curtin, *Acta Mater.* **182**, 144–162 (2020).
- S. S. Sohn, A. Kwiatkowski da Silva, Y. Ikeda, F. Körmann, W. Lu, W. S. Choi, B. Gault, D. Ponge, J. Neugebauer, and D. Raabe, *Adv. Mater.* **31**, 1807142 (2019).
- S. Guo and C. T. Liu, *Prog. Nat. Sci.: Mater. Int.* **21**, 433–446 (2011).
- C. Ng, S. Guo, J. Luan, S. Shi, and C. T. Liu, *Intermetallics* **31**, 165–172 (2012).
- Z. Lei, X. Liu, Y. Wu, H. Wang, S. Jiang, S. Wang, X. Hui, Y. Wu, B. Gault, P. Kontis, D. Raabe, L. Gu, Q. Zhang, H. Chen, H. Wang, J. Liu, K. An, Q. Zeng, T. G. Nieh, and Z. Lu, *Nature* **563**, 546–550 (2018).
- O. N. Senkov, J. M. Scott, S. V. Senkova, D. B. Miracle, and C. F. Woodward, *J. Alloys Compd.* **509**, 6043–6048 (2011).
- S. Sheikh, S. Shafeie, and Q. Hu, *J. Appl. Phys.* **120**, 164902 (2016).
- S. Guo, C. Ng, J. Liu, and C. T. Liu, *J. Appl. Phys.* **109**, 103505 (2011).
- O. N. Senkov, S. Gorsse, and D. B. Miracle, *Acta Mater.* **175**, 394–405 (2019).
- D. B. Miracle, M. H. Tsai, O. N. Senkov, V. Soni, and R. Banerjee, *Scr. Mater.* **187**, 445–452 (2020).
- J. K. Jensen, B. A. Welk, R. E. A. Williams, J. M. Sosa, D. E. Huber, O. N. Senkov, G. B. Viswanathan, and H. L. Fraser, *Scr. Mater.* **121**, 1–4 (2016).
- O. N. Senkov, J. K. Jensen, A. L. Pilchak, D. B. Miracle, and H. L. Fraser, *Mater. Des.* **139**, 498–511 (2018).
- J. P. Abriata and J. C. Bolcich, *J. Phase Equilib.* **3**, 34–44 (1982).
- A. Fernández Guillermet, *J. Alloys Compd.* **226**, 174–184 (1995).

- ²³V. Soni, B. Gwalani, T. Alam, S. Dasari, Y. Zheng, O. N. Senkov, D. Miracle, and R. Banerjee, *Acta Mater.* **185**, 89–97 (2020).
- ²⁴T. E. Whitfield, E. J. Pickering, L. R. Owen, O. N. Senkov, D. B. Miracle, H. J. Stone, and N. G. Jones, *J. Alloys Compd.* **857**, 157583 (2021).
- ²⁵T. E. Whitfield, E. J. Pickering, L. R. Owen, C. N. Jones, H. J. Stone, and N. G. Jones, *Mater.* **13**, 100858 (2020).
- ²⁶E. Pink and R. J. Arsenault, *Prog. Mater. Sci.* **24**, 1–50 (1980).
- ²⁷D. R. Trinkle and C. Woodward, *Science* **310**, 1665–1667 (2005).
- ²⁸N. I. Medvedeva, Y. N. Gornostyrev, and A. J. Freeman, *Phys. Rev. B* **76**, 212104 (2007).
- ²⁹J. R. Stephens and W. R. Witzke, *J. Less-Common Met.* **41**, 265–282 (1975).
- ³⁰A. Sato and M. Meshii, *Acta Metall.* **21**, 753–768 (1973).
- ³¹S. I. Rao, C. Woodward, and B. Akdim, *Acta Mater.* **243**, 118440 (2023).
- ³²W. D. Klopp, *Review of Ductilizing of Group VIA Elements by Rhenium and Other Solutes* (National Aeronautics and Space Administration, Washington, D.C., 1968), Vol. 4955.
- ³³Y. J. Hu, M. R. Fellingner, B. G. Butler, Y. Wang, K. A. Darling, L. J. Kecskes, D. R. Trinkle, and Z. K. Liu, *Acta Mater.* **141**, 304–316 (2017).
- ³⁴S. Laube, H. Chen, A. Kauffmann, S. Schellert, F. Müller, B. Gorr, J. Müller, B. Butz, H. J. Christ, and M. Heilmaier, *J. Alloys Compd.* **823**, 153805 (2020).
- ³⁵G. Taylor, *Prog. Mater. Sci.* **36**, 29–61 (1992).
- ³⁶F. G. Coury, Solid solution strengthening mechanisms in high entropy alloys, Ph.D. thesis, Colorado School of Mines, Golden, 2018, p. 86.
- ³⁷R. J. Arsenault, *Acta Metall.* **17**, 1291–1297 (1969).
- ³⁸A. Ghafarollahi and W. A. Curtin, *Acta Mater.* **196**, 635–650 (2020).
- ³⁹J. R. Stephens, *Metall. Trans.* **1**, 1293–1301 (1970).
- ⁴⁰S. I. Rao, C. Woodward, B. Akdim, E. Antillon, T. A. Parthasarathy, and O. N. Senkov, *Scr. Mater.* **172**, 135–137 (2019).
- ⁴¹S. I. Rao, C. Woodward, B. Akdim, O. N. Senkov, and D. Miracle, *Acta Mater.* **209**, 116758 (2021).
- ⁴²D. Caillard, M. Rautenberg, and X. Feaugas, *Acta Mater.* **87**, 283–292 (2015).
- ⁴³L. A. Gypen and A. Deruyttere, *Scr. Metall.* **15**, 815–820 (1981).
- ⁴⁴R. Labusch, *Phys. Status Solidi B* **41**, 659–669 (1970).
- ⁴⁵C. Baruffi, F. Maresca, and W. A. Curtin, *MRS Commun.* **12**, 1111–1118 (2022).
- ⁴⁶C. Lee, F. Maresca, R. Feng, Y. Chou, T. Ungar, M. Widom, K. An, J. D. Poplawsky, Y. C. Chou, P. K. Liaw, and W. A. Curtin, *Nat. Commun.* **12**, 5474 (2021).
- ⁴⁷J. Hu, H. Shen, M. Jiang, H. Gong, H. Xiao, Z. Liu, G. Sun, and X. Zu, *Nanomaterials* **9**, 461 (2019).
- ⁴⁸A. Kumar, Z. A. Ali, and B. M. Wong, *J. Mater. Sci. Technol.* **141**, 236 (2023).